



# Hypoid gear vehicle axle efficiency



I. Kakavas\*, A.V. Olver, D. Dini

*Tribology Group, Department of Mechanical Engineering, Imperial College, London, UK*

## ARTICLE INFO

### Article history:

Received 6 January 2016

Received in revised form

19 April 2016

Accepted 25 April 2016

Available online 3 May 2016

### Keywords:

Elastohydrodynamics

Lubrication

Friction

Contact mechanics

Hypoid gear

## ABSTRACT

In this paper, a study of a hypoid gear vehicle axle is presented. Using a custom rig, load-independent losses have been accurately measured and the effect of viscosity on spin loss has been quantified. Solution methods for the calculation of component losses are presented and combined into a complete thermally coupled transient model for the estimation of axle efficiency. An analysis of hypoid gear kinematics reveals a simplification, commonly adopted by other researchers, regarding the velocity of the point of contact in hypoid gears, to be in error. As a result, the calculation of lubrication parameters has been improved. Finally, experimental measurements are compared to the generated simulation results for a number of operating scenarios and satisfactory correlation is observed.

© 2016 Elsevier Ltd. All rights reserved.

## 1. Introduction

The increasing global energy demand combined with environmental concerns, as well as the volatile value of crude oil [1] has driven governments and markets to pursue higher efficiency in the automotive industry through incentives and legislation [2]. In the average passenger vehicle, around a third of the fuel is transformed into mechanical energy, while the rest escapes the system through high exhaust gas enthalpy and cooling. Although most of the mechanical energy consumption is utilised in overcoming driving resistances, a significant part is wasted in engine and transmission losses [3].

Transmissions and differential axles share the same core energy consuming components, i.e. gear pairs and rolling element bearings. Efficient powertrain design heavily depends on a thorough understanding of the operating behaviour of such components. Spur and helical gear pairs, common in vehicle gearboxes, have been extensively studied and a number of loss estimation methods have been proposed [4–9]. In differential axles gear pairs with more complicated geometry, such as spiral bevel and hypoid gears, need to be used to achieve transmission of power through a right angle. Hypoid gears can offer higher load capacity and quiet operation for a small efficiency compromise, making them attractive to axle manufacturers [10]. On the downside, the complex geometry of hypoid gears has delayed the development of reliable tools for efficiency estimation tools. Recent work on hypoid gears involves contact models that require a great number

of input parameters, extending to tooth cutting [11] or depending on separate software packages [12]. In this study, hypoid gear vehicle axle losses have been quantified through experimental measurement and a simple axle efficiency estimation method is proposed.

## 2. Experimental set-up

The losses generated in a vehicle axle can be categorised as load-dependent or load-independent (Fig. 1). Load-dependent losses (e.g. those due to contact friction) arise when load is transferred in the contact of rough surfaces in relative motion and are the result of the interaction of lubricated rough surfaces [13]. In addition to the effect of load, the rolling and sliding velocities of the surfaces, as well as the lubrication regime, are defining parameters for the estimation of load-dependent losses. Load-independent losses (often referred to as spin losses) are mostly associated with fluid–surface interaction. More specifically, spin losses are the combination of oil churning and windage loss in the immersed revolving system and are not affected by contact loads [4]. Additional auxiliary losses (e.g. seal loss) are also included in the load-independent category.

The total axle losses as a function of torque and temperature may be measured, for example, using a dynamometer together with torque metres on input and output shafts. When no output torque is applied, the input torque may be too low for accurate measurement with a torque metre. Here, a rig based on the inertia run-down method has been utilised (Fig. 2). The rig mainly consists of an electric motor, a clutch, an axle base and instrumentation. The axle is mounted on the base and connected to the electric

\* Corresponding author.

E-mail address: [i.n.kakavas@gmail.com](mailto:i.n.kakavas@gmail.com) (I. Kakavas).

**Nomenclature**

$A$	Vehicle frontal area
$A_{axle}$	Axle frontal area
$C_D$	Coefficient of drag
$C_p$	Heat capacity
$C_{rolling}$	Coefficient of rolling friction
$D_0$	Deborah number
$F_r$	Froude number
$G_e$	Elastic shear modulus
$Nu$	Nusselt number
$Pr$	Prandtl number
$Re$	Reynolds number
$R_{pitch}$	Pitch radius
$S$	Non-dimensional strain rate
$S_m$	Gear immersed area
$T_t$	Temperature of lumped mass at $t$
$T_{ch}$	Churning torque loss
$T_{env}$	Environmental temperature
$T_{transmitted}$	Transmitted torque
$V_{lub}$	Lubricant volume
$a$	Pressure–viscosity coefficient
$a_t$	Thermal diffusivity
$b$	Gear thickness
$g$	Gravitational acceleration
$h$	Heat transfer coefficient
$h_{lub}$	Lubricant immersion
$k_m$	Rotating component inertia factor
$m_e$	Axle equivalent lumped mass

$\mathbf{n}_{g,p}$	Gear or pinion velocity normal to the contact plane
$\bar{p}$	Mean pressure in contact
$t$	Time
$\mathbf{u}'_c$	Component of the velocity of the point of contact on the contact plane perpendicular to the line of contact
$\mathbf{u}_e$	Entrainment velocity
$\mathbf{u}'_{g,p}$	Component of the gear or pinion tooth velocity on the contact plane perpendicular to the line of contact
$\mathbf{u}_{g,p}$	Gear or pinion tooth velocity on the contact plane
$\mathbf{u}_s$	Sliding speed
$u_{veh}$	Vehicle speed
$\mathbf{v}_{g,p}$	Gear or pinion tooth velocity
$\Omega$	Contact plane
$\dot{\gamma}$	Strain rate
$\eta_0$	Dynamic viscosity
$\lambda$	Lambda ratio
$\mu$	Friction coefficient
$\mu_b$	Coefficient of boundary friction
$\nu$	Kinematic viscosity
$\rho$	Density
$\bar{\tau}$	Mean shear stress in contact
$\bar{\tau}^*$	Non-dimensional shear stress
$\tau_c$	Limiting shear stress
$\tau_c^*$	Non-dimensional limiting shear stress
$\tau_E$	Eyring stress
$\phi_{ish}$	Shear heating coefficient
$\phi_{rs}$	Starvation coefficient
$\omega$	Angular velocity

motor through the clutch. By varying the power of the electric motor, the axle is accelerated to a desired speed. The clutch is then disengaged and the axle is allowed to decelerate naturally due to losses occurring in the rotating axle components. The rotational speed of the axle is constantly monitored using an optical encoder

attached to the crown gear shaft. The captured rate of deceleration ( $d\omega/dt$ ) is then converted to instantaneous axle torque loss ( $T$ ), given the rotational inertia of the axle ( $I$ ). A flywheel has been attached to the input flange of the rear drive unit. This increases the total effective rotational moment of inertia to  $I=0.035 \text{ kg m}^2$  (referred to the high-speed shaft) prolonging the run-down period and serving to increase the time-resolution of the torque determination, particularly at low speeds. The differential gears of the axle were fixed with structural adhesive in order to ensure the two output shafts were synchronised.

In order to identify the relationship between viscosity and axle loss generation, lubricants of different viscosity (but with the same chemical additive package and base-stock type) have been used. The temperature of the oil sump is monitored prior to run-down initiation. In each case, standard production oil volume has been used allowing all four bearings and lower gear teeth to be sufficiently immersed (Fig. 3). The starting speed of the rundown was set to 2000 rev/min. Measurements were also conducted for 1000 and 500 rev/min in order to identify potential differences due to flow behaviour. Each test was run several (3–4) times to establish repeatability and a sixth-order polynomial is produced from the average values (Fig. 4).

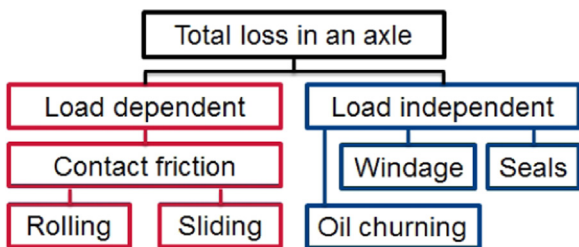


Fig. 1. Axle losses categories.

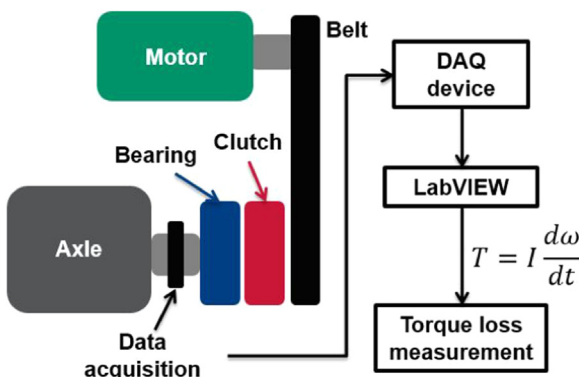


Fig. 2. Methodology of spin loss measurement.

**3. Axle simulation**

3.1. Transient model

As displayed in Fig. 5, the basic structure of the model consists of the initial parameter input, the theoretical component loss estimation, the heat transfer calculation and, finally, the axle loss/efficiency output. The transient component of the algorithm can

Download English Version:

<https://daneshyari.com/en/article/7002562>

Download Persian Version:

<https://daneshyari.com/article/7002562>

[Daneshyari.com](https://daneshyari.com)